



Fabrication of superhydrophobic aluminium alloy surface by twice nanosecond laser scanning

Yanling Wan , Lining Xu, Huadong Yu

College of Mechanical and Electric Engineering, Changchun University of Science and Technology, Changchun 130022, People's Republic of China

 E-mail: wanyl@cust.edu.cn

Published in *Micro & Nano Letters*; Received on 13th July 2017; Revised on 5th December 2017; Accepted on 8th December 2017

The superhydrophobic surface of aluminium alloy was fabricated by nanosecond laser facility. The surface structures of the specimen were observed by scanning electron microscope and confocal laser scanning microscope. Surface hydrophobicity was evaluated by contact angle of deionised water. The phases present in the aluminium alloy surface were identified by X-ray energy spectrum analysis module of scanning electron microscope. The study showed that, a simple method of the fabrication of superhydrophobic aluminium alloy surface by twice nanosecond laser scanning, can make bowl like micro-nano structure on the surface of specimen. Compared with the contact angle of 140.21 degrees, which of sample surface with groove structure obtained by using once nanosecond laser scanning, the contact angle of the sample surface prepared by twice nanosecond laser scanning can up to 154.36 degrees. On the as-obtained sample surface, there is the hydrophobic substance containing more oxygen element, because of the coupling effect of laser and material. The surface roughness is related to the depth of the microstructure, and has no clear relationship with the surface wettability. Therefore, it is speculated that the joint action micro-nano structure and hydrophobic elements made the surface of aluminium alloy show super hydrophobicity.

1. Introduction: Usually, when the surface contact angle is $>150^\circ$, it is defined as superhydrophobic surface [1]. Studies have shown that superhydrophobic surface has broad application prospects in oxidation resistance, anti-fog, anti-corrosion, waterproof, snow prevention, antifouling, self-cleaning and other fields [2–5]. In recent years, the preparation and application of superhydrophobic surfaces have been widely developed, and a large number of experiments show that the realisation of the superhydrophobic surface is a common effect of the rough structure and low surface energy material [6]. There are a number of different methods to prepare the superhydrophobic surface, including electrospark wire-electrode cutting, laser etching, electro-spinning, anodic oxidation, layer-by-layer deposition and the sol-gel process. Among them, the laser etching method has the advantages of stable processing performance, low cost, simple operation and no use of dangerous or expensive chemical reagents.

Laser technology has been developed rapidly since its appearance. It has been widely used in surface micromachining because of its high efficiency, stability, reliability and long life. However, femtosecond laser with the most excellent performance has a high cost, accordingly, it is of important realistic significance to study the application of nanosecond laser with low processing cost [7]. In this Letter, the microstructure of sample surface was fabricated by using nanosecond laser equipment. After once nanosecond laser scanning, the as-obtained sample surface with groove structure showed hydrophobicity. Finally, after twice nanosecond laser scanning, the machined sample surface with special microstructure had superhydrophobicity. This processing method is simple to operate and can process metal material with stable processing effect. Hydrophobic elements are present on the as-obtained sample surface without chemical modification.

2. Materials and methods

2.1. Materials: The material of the experimental sample was 7075 aluminium alloy plate, and its dimension was 20 mm \times 20 mm \times 2 mm. Before the start of the experiment, the specimens were polished by polishing machine, using 400#, 600#, 1000#, 2000# grit SiC paper, respectively.

Experimental reagents: deionised water.

2.2. Methods: In a typical scanning optical system, first, the laser beam passes through two rotating lenses, which can change the direction of the laser beam, and then, focusing the laser beam with a lens. The rotating shafts of the two lenses are perpendicular to each other. The lens can make the laser beam focus on any point in the working area. This is what is known as the 'laser scanning' working area.

A specimen was placed on the worktable. Then, the focal plane of the laser device was adjusted to the sample surface, and equidistant straight lines were drawn in operation interface and the spacing was 50 μm . There were two steps to fabricate the microstructure on the sample surface. The specimen was first processed with the following parameters, respectively: power was 16 W, three pulses and scanning speed was 500 mm/s. Then, after the laser machining for the first time, the scanning speed was changed into 1000 mm/s, and finally the superhydrophobic aluminium alloy surface was obtained through the machining for the second time.

Post-processing was required, that is, to remove the surface slags of fabricated sample. There were many slags on the surface of the sample after laser ablation, which were a kind of oxide formed at high temperatures after vapourisation of the material surface. Therefore, a simple cleaning scheme was selected, the specimen was ultrasonically cleaned for 10 min in deionised water and dried naturally at room temperature.

2.3. Performance test and result representation: The surface profile of the specimen was obtained by laser scanning confocal microscope and scanning electron microscope (EVO MA25).

The water contact angle was used to evaluate wettability of the specimen surface, and it was tested using optical contact angle measuring device (OCA20, German Dataphysics company). In order to guarantee the accuracy of the surface data of the treated sample, the treated aluminium alloy samples were cleaned with deionised water by ultrasonic for 5 min, and then dried at room temperature. The above procedure shall be completed prior to contact angle measurement. Surface hydrophobicity was obtained using the mean value of the contact angles of three different positions of each sample, and the volume of deionised water drop was 4 μl .

3. Results and discussion

3.1. Surface wettability: Optical contact angle measuring device was used to measure the surface of the aluminium alloy. The results showed that the static contact angle of water droplets on the surface of the smooth aluminium alloy was about 76.4° (Fig. 1a). After the first laser machining, the hydrophobicity of fabricated Al alloy surfaces was greatly improved, and the maximum contact angle reached 140.21° (Fig. 1b). Furthermore, after the second laser machining, the static contact angle of the specimen reached $154.36^\circ (\pm 0.5^\circ)$ (Fig. 1c), which means we had got the surfaces with superhydrophobicity.

Through the machining of first scanning of the nanosecond laser, groove structures were formed on the sample surface, and the wettability of aluminium alloy specimens changed from hydrophilic surface to hydrophobic surface. After the machining of second scanning of the nanosecond laser which had changed the processing parameters, the wettability of aluminium alloy specimens changed from hydrophobic surface to superhydrophobic surface. The microstructures of the aluminium alloy after the first laser scanning and the second laser scanning must be different. It can be seen that the change of microstructure can affect the wettability of aluminium alloy surface.

3.2. Surface morphology: Scanning electron microscopy and laser-scanning confocal microscopy were used to show the profile of the specimens, it can be seen that the surfaces of both once laser machining and twice laser machining appeared numerous sub-micron and nanometre-sized slags, and there was a smoother bottom in the pit. The groove structure formed on the surface of the aluminium alloy after the once nanosecond laser scanning (Fig. 2), and the projection profile of which was a micron-sized structure. Furthermore, there were also numerous sub-microscale and even nanoscale slags piled up on the bulge, made the surface of the specimen form a double scale structure. This dual-scale microstructure facilitates trapping of air and formation of three-phase contact lines, and the shape, length and continuity of contact lines are the important factors that affect the adhesion of the surface. In general, the smaller the three-phase contact line is, the easier the droplets are to roll on the solid surface, and the solid surface shows a low adhesion state [8]. The concave part of the groove was relatively smooth can trap more air, nevertheless,

the solid contact area was relatively small and did not support the droplets very well.

Compared with the groove structure, the structure of aluminium alloy surface fabricated by twice laser machining (Fig. 3) was more rough, and had more slags on the bulge that made its height more higher. It was observed that the inside and bottom of the micro-pit are very smooth, and there were micro-/nano-sized partitions formed between the micro-pits due to the gasification and condensation of aluminium alloy material during the laser machining, which was beneficial to support small water droplets. To observe the as-prepared sample surface morphology integrally, this morphology was similar to that of the bowl-like structures, at the same time, there were countless regularly arranged pyramid-like structures. It can be surmised that, this special morphology and micro-/nano-sized structure achieved the superhydrophobic property of sample surface.

3.3. Surface roughness: In order to study the influence of different roughnesses and wettability, to change the number of pulses so that the depth of the microstructure can be controlled according to the target value, and finally the surface roughness was changed.

Five groups of polished specimens were put on the work bench, and equidistant straight lines were drawn in operation interface and the spacing was $50\ \mu\text{m}$. Except the number of pulses, the other values of processing parameters were the same, the machining values are shown in Table 1.

The optical contact angle measuring instrument was used to test the surface of as-obtained specimens. The roughness was measured by using the Mahr surface roughness and outline admeasuring. Based on the summarisation of experiment data, Table 2 and line chart were obtained.

To observe the line chart (Fig. 4), it can be seen that, the greater the depth of groove was, the greater the corresponding roughness value became. However, there was no linear relationship between contact angle and surface roughness. Under the coupling effect of nanosecond laser and aluminium alloy, the groove depth became deeper with the increasing pulse number, and the value of the roughness was determined by the undulating contours of the surface, so that the increase of pulse number made the roughness value became bigger.

3.4. Material composition: The X-ray energy spectrum analysis module of scanning electron microscope (EVO MA25) produced

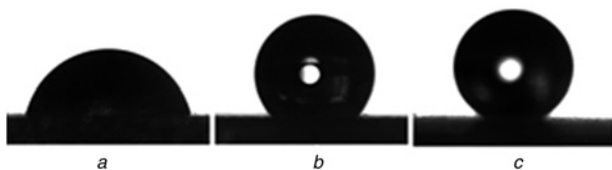


Fig. 1 Water contact angles of obtained aluminium alloy samples
a Smooth aluminium alloy
b Aluminium alloy processed with once laser machining
c Aluminium alloy processed with twice laser machining

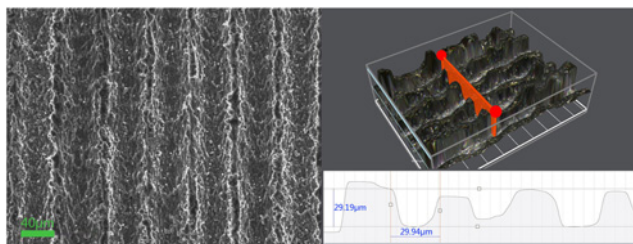


Fig. 2 Surface morphology of once laser machining

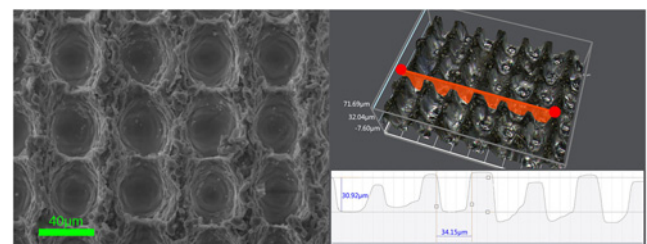


Fig. 3 Surface morphology of twice laser machining

Table 1 Processing parameters

Group	Power, W	Scanning speed, mm/s	Pulse number
1	16	500	3
2	16	500	4
3	16	500	5
4	16	500	6
5	16	500	7

Table 2 Experimental values of contact angle and roughness

Pulse number	Contact angle, deg	Roughness (Ra), μm	Groove depth
3	138.23	3.02	9.23
4	137.51	3.34	18.36
5	124.36	3.87	42.86
6	140.21	4.11	59.31
7	130.22	4.34	65.10

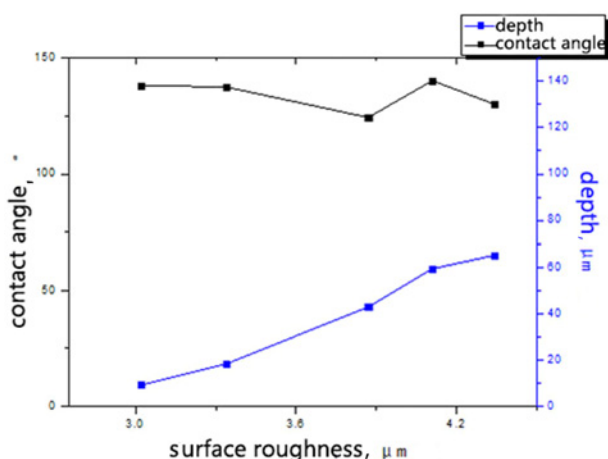


Fig. 4 Line chart of contact angle and roughness

by the German Zeiss Company was used to test the composition of the specimen. 7075 aluminium alloy is a kind of aviation superhard aluminium material, and its main components are aluminium, zinc, magnesium and copper. The polished specimens, once laser machined specimens and twice laser machined specimens were analysed by the X-ray energy spectrum analysis module.

The spectrogram of polished specimens without laser processing (Fig. 5) showed that, besides the inherent metallic elements of aluminium alloy, it contains very little oxygen element, which means that the surface has a substance containing oxygen element. The content of oxygen element of once laser machined samples (Fig. 6) changed from 1.27 to 4.61%, and its surface morphology was shown in Fig. 2. Compared with once laser machined sample, the surface oxygen content of the twice laser machined sample (Fig. 7) changed from 4.61 to 9.26%, Fig. 3 is its surface morphology. It can be speculated, during the process of laser machining, a large amount of vapourised slags reacted with oxygen and occurred severe oxidation reaction, and then it splashed on the surface, so that there was an increase of oxygen content

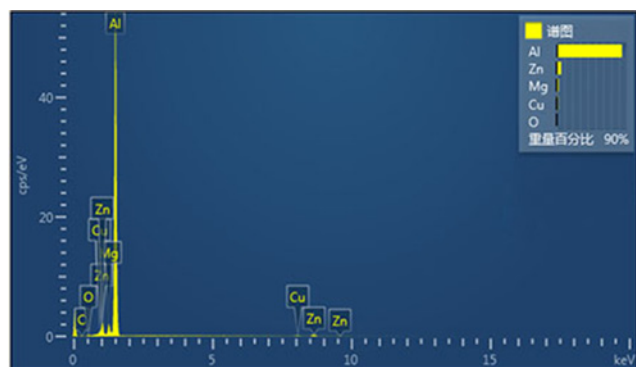


Fig. 5 X-ray energy spectrum of aluminium alloy matrix

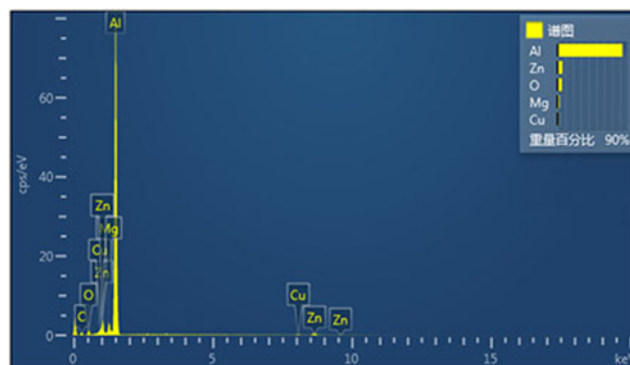


Fig. 6 X-ray energy spectrum of once laser machined aluminium alloy

after once laser machining. The twice scanning led to repeated processing, and the accumulation of slags made its height became higher and countless regularly arranged pyramid-like structures and the partition between the bowl-like structures formed, therefore, there was the increasing number of surface area of slags and the oxygen content. At the same time, oxygen is also a hydrophobic element, this is consistent with the better hydrophobicity of the twice laser machined specimens. Additionally, X-ray diffraction analysis of samples was obtained. In the aluminium alloy matrix, the oxygen carrier was MgAl_2O_4 and $\text{Al}_{17.74}\text{Cr}_{1.25}\text{Fe}_{2.19}\text{Mg}_{8.08}\text{Ni}_{0.08}\text{O}_{40}\text{Si}_{0.01}\text{Ti}_{0.04}\text{Zn}_{0.02}$ exist in the laser machined specimens. It can be inferred that the laser machining caused a strong oxidation reaction and produced $\text{Al}_{17.74}\text{Cr}_{1.25}\text{Fe}_{2.19}\text{Mg}_{8.08}\text{Ni}_{0.08}\text{O}_{40}\text{Si}_{0.01}\text{Ti}_{0.04}\text{Zn}_{0.02}$, and this substance led to the increase of oxygen element content of surface and the property of anti-water.

3.5. Analysis of the mechanism of superamphiphobic surface: To study the microstructure of groove surface, it is found that repeated processed area is bound to appear in the process of machining, and this leads to a cumulative effect on repeated processing areas. This cumulative effect comes from two aspects in the concrete process, on the one hand, during the laser processing process, processing area of adjacent two pulses has an overlapping part, on the other hand, an increase in the number of pulses leads to repeat machining. The effect of the cumulative effect is the increase of the groove depth, this increase in depth will cause more vapourised materials to condense on the surface and more slags accumulate on the sample. The accumulation of slags on the sample surface in the preparation of microstructures brings two benefits, first, sub-microscale or even nanoscale slags have been appeared on the micro-sized structures, second, a large number of slags that accumulate on the surface increase the

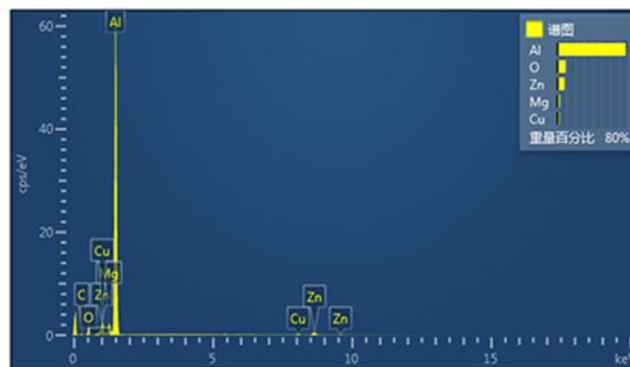


Fig. 7 X-ray energy spectrum of twice laser machined aluminium alloy

microstructure's height, which benefits for trapping more air and increasing the surface area of microstructure.

The change of surface composition of aluminium alloy during processing was observed. With the increase of the number of laser machining, the content of oxygen also increases. According to the change of surface microstructure, the number of slags and the surface area of the microstructure were increasing, this facilitates the increase of the surface oxygen content. The laser beam not only heats the surface of the material, but also continues to melt the surface. After the process of workpiece surface melting by laser beam, when metal is cooled, a surface layer of grain refinement is formed on the surface, its distribution of phase is more uniform and the grain is finer, as a result, the properties of the surface layer are quite different from those of the unprocessed sample surface [9].

After coupling between nanosecond laser and aluminium alloy, both the bowl-like structures and regularly arranged pyramid-like structures formed on the surface are micro/nanostructures, and the change of surface material composition results in the existence of more hydrophobic elements on the surface. To combine the above research results and classical theory of wettability, it can be speculated that, the above two reasons make the processed sample conform to the Cassie-Baxter (CB) model theory [1], and the CB model can be used to explain the phenomenon of the superhydrophobic surface of the specimen after coupling.

4. Conclusion: In this Letter, twice nanosecond laser scanning was performed on the surface of aluminium alloy by nanosecond laser processing equipment. Changes in the composition of the surface material can occur without chemical modification, and that makes the sample surface obtain hydrophobic property. Compared with the surface of once laser machined sample, the bowl-like structures and regularly arranged pyramid-like structures formed on the surface of twice laser machined sample, which makes the surface area become larger and hydrophobic effect become better. It is speculated that remelting occurs during the twice laser scanning, and it leads to the changes of crystal structure inside the material, this is more favourable for surface hydrophobic

effect. Under the coupling of nanosecond laser and metal material, the roughness increases with the depth of the microstructure, however, there is no definite correlation between roughness and surface wettability. It is proved that the surface of aluminium alloy with superhydrophobic property can be prepared by using only nanosecond laser with lower cost and stable processing effect.

5. Acknowledgments: This work was supported by China-EU H2020 International Science and Technology Cooperation Programme (FabSurfWAR grant nos. 2016YFE0112100 and 644971), Lu Quan Innovation Foundation of College of Mechanical and Electric Engineering, Changchun University of Science and Technology of China.

6 References

- [1] Zhao K., Liu K.S., Li J.F., *ET AL.*: 'Superamphiphobic cali-based bulk metallic glasses', *Scr. Mater.*, 2009, **60**, (4), pp. 225–227
- [2] N. A., H. K., W. T., *ET AL.*: 'Preparation of transparent superhydrophobic boehmite and silica films by sublimation of aluminum acetylacetonate', *Adv. Mater.*, 1999, **11**, (16), pp. 1365–1368
- [3] Barthlott W.: 'Purity of the sacred lotus, or escape from contamination in biological surfaces', *Planta*, 1997, **202**, (1), pp. 1–8
- [4] Nakajima A.: 'Design of a transparent hydrophobic coating', *Nippon Seramikkusu Kyokai Gakujutsu Ronbunshi*, 2004, **112**, (1310), pp. 533–540
- [5] Zhang H., Lamb R., Lewis J.: 'Engineering nanoscale roughness on hydrophobic surface – preliminary assessment of fouling behaviour', *Sci. Technol. Adv. Mater.*, 2005, **6**, (3–4), pp. 236–239
- [6] Jafari R., Farzaneh M.: 'Fabrication of superhydrophobic nanostructured surface on aluminum alloy', *Appl. Phys. A, Mater. Sci. Process.*, 2011, **102**, (1), pp. 195–199
- [7] Groenendijk M.: 'Fabrication of super hydrophobic surfaces by Fs laser pulses', *Laser Tech. J.*, 2008, **5**, (3), pp. 44–47
- [8] Lai Y.K., Chen Z., Lin J.C.: 'A review on the recent progress in superhydrophobic surfaces with special adhesions', *Sci. Sin., Chim.*, 2011, **41**, (4), pp. 609–628
- [9] Tang M.: 'Laser ablation of metal substrates for super-hydrophobic effect', *J. Laser Micro*, 2011, **6**, (1), pp. 6–9